Distinct routes to thermotolerance in the fungal pathogen *Cryptococcus neoformans*

Mara J. W. Schwiesow[1,2†], Nels C. Elde[1,2], Zoë A. Hilbert[1-3*]

[1]Department of Human Genetics, University of Utah, Salt Lake City, UT 84112 , USA
[2] Howard Hughes Medical Institute, Salt Lake City, UT, USA
[3]Department of Biology, Boston College, Chestnut Hill, MA 02467, USA
[†]Current address: Department of Molecular and Cellular Biology, University of California at Merced, Merced, CA, USA

*Correspondence: hilbertz@bc.edu

Abstract

Increasing temperatures associated with climate change have the potential for far-reaching impact on human health and disease vectors, including fungal pathogens. Pathogenic fungi occupy a wide range of environments across the world, and their ranges have been slowly expanding in recent decades due, in part, to climate change. Despite these links between increasing temperature and higher prevalence of fungal disease, the direct effects of rising environmental temperatures on the evolution of pathogenic fungi remains unclear. In this study, we investigated how increasing temperatures drive adaptive evolution in the human fungal pathogen *Cryptococcus neoformans*. First, we performed serial passages of a *C. neoformans* environmental isolate with gradual changes in temperature over the course of ~40 days. Through this approach we identified several distinct thermally adapted isolates with competitive growth advantages over the parental strain at high temperatures. We then characterized the phenotypic and genetic changes acquired in several evolved isolates, which include alteration of cell size, colony morphology, and, surprisingly, antifungal resistance. These results highlight the remarkable flexibility of fungi to adapt rapidly to new environments and raise pressing questions about the impacts of rising environmental temperatures on the future of infectious diseases and human health.

Introduction

The impacts of planetary warming on biological systems hold pivotal implications for human and animal health worldwide[1]. Climate change is likely to have particularly dramatic effects in the realm of infectious disease, where increased environmental temperatures could fundamentally alter the range, number, and nature of pathogenic microbes, such as fungi[2]. However, little work has been done to investigate how incrementally increasing temperatures will affect the evolution of these pathogens and what consequences this adaptation may have in the context of human infection.

For fungi, in particular, the inability of most species to grow at the high body temperatures characteristic of mammals has long been considered a primary limiting factor in the ability of these microbes to establish infection[3]. As global temperatures rise, however, adaptation to higher temperatures is expected to drive increases in the number of fungal species capable of surviving at mammalian body temperature, perhaps even driving the emergence of new species with pathogenic potential. Increased environmental temperature will also result in range expansions for pathogenic fungi. Indeed, this has already been observed in several fungal species including *Coccidioides* spp., *Cryptococcus gattii*, and *Candida auris*, with *C. auris* emerging on three separate continents simultaneously[4–6]. Although changes in the geographic range for these particular species are in part due to expansion of their preferred environments, there is also evidence to suggest that these organisms are adapting to new, more stressful environmental conditions[7,8]. Given these trends, it can be expected that as global temperatures continue to rise, the ranges of these and other pathogenic fungi will only continue to expand, the threat of thermal adaptation in these organisms will escalate, and human body temperature may no longer pose such an impediment to fungal infection.

In this study, we focus on the role of increasing environmental temperatures in shaping the evolution of the common human fungal pathogen, *Cryptococcus neoformans*. *C. neoformans* is a pathogenic basidiomycete fungus found ubiquitously in the environment, usually residing in bird guano, soil, and trees, and infection by this species is currently estimated to cause over 100,000 deaths annually[9,10]. Strains of *C. neoformans* occupy a wide range of temperature environments having been isolated from all continents, excluding Antarctica, both from environmental and clinical settings[11–15]. However, our understanding of how thermotolerance evolved in this species and may vary across strains is relatively limited.

Some studies of laboratory reference isolates have revealed candidate genes and pathways in *C. neoformans* that are important for success at high temperature. For example, heat shock proteins, and certain other conserved genetic pathways, such as *CDC11* and the HOG pathway, all play roles in adaptation to the host environment, including adaptation to host temperature[16–19]. However, these studies largely focus on gene knockouts in the laboratory strain background and obscure a more realistic view of how this organism might adapt by modulating expression or function of these or other genes to survive under changing conditions. Using both the genetic and phenotypic diversity of the large collections of environmental and clinical isolates of *C. neoformans* might reveal some of the adaptation strategies this species employs; we can also use experimental methods to study adaptation to particular environmental conditions in the lab in order to better understand these processes.

Experimental evolution is a powerful tool to investigate the processes and mechanisms of adaptation to new environments in wide-ranging species. Studies of thermal adaptation, in particular, include the pioneering work of Bennett and Lenski, who used long-term experimental evolution to study the adaptive changes that occur in the bacterial species *Escherichia coli* under high temperature stress[20]. In fungal species, similar serial passaging approaches at consistent, high temperatures have proven powerful in generating heat-tolerant strains for use in industrial settings[21]. Additionally, two studies in the yeasts *Saccharomyces cerevisiae* and *Saccharomyces uvarum* have shown that gradual and stepwise temperature ramps can increase the thermotolerance of fungi by 1.5°C or more, suggesting that these fungi have a

remarkable plasticity for tolerating temperature fluctuations[22,23]. However, studies exploring the thermal adaptation capabilities of environmental pathogenic fungi and related impacts on pathogenicity have been largely missing.

In this study, we leverage experimental evolution approaches to study the process of thermal adaptation in the clinically relevant *C. neoformans*. Through gradual exposure to increasing temperatures over many generations, we found that not only can *C. neoformans* adapt to produce genetically distinct strains with increased thermotolerance, but that this adaptation occurs on relatively short timescales. In only 38 days of continuous culturing, we observed increased thermotolerance of one environmental strain of *C. neoformans* characterized by improved growth at high temperature with clear fitness advantages over the parental strain. Thermal adaptation occurred across a range of media types and correlates with other phenotypic changes in cell size, colony morphology, and antifungal resistance. Our findings indicate that *C. neoformans* is capable of adapting to increasing global temperatures and provide a foundation on which to build an understanding of how our changing climate will impact human health and fungal disease.

Results

Variable thermotolerance across environmental isolates of *C. neoformans*

Environmental strains of *C. neoformans* occupy diverse locations and are exposed to a variety of temperature ranges with varying nutrient availability. While environmental isolates may generally experience more temperate climates, they are also likely subjected to wider temperature swings in contrast to clinical isolates, which are better able to grow at the high temperatures (37°C and above) of the human body. To test the thermotolerance properties of a panel of environmental *C. neoformans* isolates, we performed spot dilution assays and assessed the growth of these strains at two different temperatures: the standard laboratory culture temperature of 30°C and at a high temperature of 37°C, representative of human body temperature. Assays were performed under two distinct nutrient conditions: strains were assessed for growth on Yeast extract Peptone Dextrose (YPD), a rich media, as well as on Yeast Nitrogen Base (YNB) with glucose, a more minimal and chemically defined media to assess how thermotolerance might differ across these different nutritional environments.

These assays revealed that among environmental isolates, thermotolerance varies widely, even between closely related strains (Figure 1). Some strains, such as Ftc217-1 and Jo278-1, grow well at high temperature, similar to the laboratory reference strain, H99 (Figure 1B and C). Others, like Muc387-1, exhibited moderate growth defects at high temperature. In general, growth differences at both temperatures were more pronounced on the minimal YNB media than on YPD.

Among the set of strains tested here, one environmental isolate stood out: Ftc239-1. This strain, which was isolated from a mopane tree in Botswana, is closely related to Ftc217-1, but displays strikingly different growth across temperatures and nutrient conditions[13,14]. Unlike Ftc217-1, Ftc239-1 has severely attenuated growth at 37°C on both YNB and YPD. This strain also displays decreased growth at 30°C on YNB media (Figure 1B). Although the growth of Ftc239-1 at 30°C on YPD was less obviously diminished, we did note that the colonies were smaller than those of the reference strain or other strains tested (Figure 1C). The difference in growth on these two media types, across all strains tested but particularly in Ftc239-1, suggests that thermotolerance and nutrient conditions interface to control fungal growth.

Given the severe growth defects of Ftc239-1 at high temperatures, we reasoned that this would be an ideal strain to use to explore the mechanisms by which thermotolerance evolves in this species. In particular, the phenotypes of this strain gave us an opportunity to explore how it might adapt to higher temperatures relevant for human infection, while also providing an avenue to investigate the role of nutrient conditions in thermal adaptation.

Experimental evolution drives fungal adaptation to increasing temperatures

We used laboratory-based experimental evolution to study the process of thermal adaptation in the Ftc239-1 *C. neoformans* strain. Although temperature increases associated with human-induced climate change are rapid for geologic time, they are much more gradual for the organisms experiencing those changes. As such, we designed our experimental evolution paradigm to mimic the gradual temperature increases environmental pathogens may experience in the coming decades, though over a greatly abbreviated timescale. Specifically, Ftc239-1 was serially passaged starting at 30°C with temperature increases of 0.5-1°C every 4 to 6 days until a temperature of 35°C was reached (Figure 2A). From the originating culture of Ftc239-1, eight populations were evolved in parallel, with four passaged in a rich media environment (YPD) and four passaged under nutrient-limiting conditions (YNB). These independently evolving Thermal Adaptation populations were named TA1-4 for the populations evolved in YPD and TA5-8 for the YNB-passaged replicates (Figure 2A).

All of the populations were viable until the end of the evolution experiment (35°C), indicating that this *C. neoformans* strain has the ability to adapt to or at least withstand increased thermal stress. Following the end of passaging, we harvested and froze the evolved populations, and also recovered individual clonal isolates for further characterization. Intriguingly, we observed variation in the appearances and morphology of the clonal samples at the end of the evolution. Some displayed a mucoid appearance, while others had increased colony size compared to the starting isolate, providing our first indication that our experimental evolution had yielded new and potentially adaptive phenotypes in these populations (Supplemental Tables 1 and 2). Further, changes in these phenotypes were not always universal within populations, suggesting that there was both phenotypic and genetic heterogeneity at the end of our course of evolution.

Experimentally evolved isolates grow better on solid media at high temperatures

Following passaging, we first set out to determine whether any of the individual endpoint colonies displayed increased growth at high temperature compared to the parental strain. We, again, employed spot dilution assays to assess the growth phenotypes of our 36 recovered isolates (Supplemental Figure 1). These experiments revealed three isolates from two independent populations as displaying a robust increase in their ability to grow at 35°C (Figure 2B and C). One of these isolates was evolved in YPD (TA1-1) and two of them were evolved in YNB (TA8-2 and TA8-3).

At 30°C, TA1-1 had increased growth on YNB, while maintaining similar growth on YPD as the parental strain (Figure 2B and C, inner panels). TA8-2 and TA8-3, which are derived from the same TA8 population, grew similarly to the parental strain at 30°C. At 35°C, however, all three evolved isolates grew one or two dilutions further than the parental strain. This effect was consistent on both media types suggesting that thermotolerance in these isolates confers an advantage across nutrient conditions. Many of the other endpoint colonies grew similarly to the parental strain at both temperatures, though there was variation between isolates and between populations (Supplemental Figure 1).

We next tested whether the increased thermotolerance in our strains conferred an enhanced ability to grow at high temperatures beyond the range of our evolution and whether there are tradeoffs for increased thermotolerance, perhaps affecting growth at temperatures below 30°C. Thermal adaptation studies with other microbial species, like *E. coli*, have suggested that such paradigms can select for evolved isolates with highly specific temperature preferences – optimized for growth at the temperatures using during the experiment[20]. To assess the growth phenotypes of our strains outside the bounds of the experimental evolution, we looked at growth of our selected isolates in parallel at 26, 30, 35 and 37°C. All three thermally-adapted isolates showed increased growth at 37°C on both YPD and YNB medias (Figure 2B and C, outer panels). There was no substantial difference in growth from the parental

strain for any isolates at 26°C on YPD, however there was a slight increase in growth of the evolved strains on YNB at this temperature. These results suggest that the gradual adaptation of this *C. neoformans* strain to a specific high temperature (35°C) confers a growth advantage in high temperatures generally, with no apparent tradeoffs for growth at lower temperatures.

Thermally adapted strains outcompete the parental strain at 35°C

The clear differences in growth between our evolved isolates and the parental strain revealed by spot assays hint at potential fitness advantages in the evolved isolates. To directly test whether the evolved strains gained a fitness advantage for growth at high temperature, we conducted co-culture competition experiments. In these competition experiments, evolved strains were grown together with a drug-resistant version of the parental strain in the same liquid media they were originally evolved in (Figure 3A).

These experiments revealed that each of the three evolved strains has a substantial competitive advantage over the parental strain at 35°C. TA1-1 grew over five times better than the parental strain, and TA8-2 and TA8-3 each had a three to four-fold advantage in their respective medias (Figure 3B and C). While this fitness effect is less robust at 30°C, the competitive advantages of the evolved strains were maintained at lower temperatures as well. These data suggest that the evolved isolates, through incremental temperature increases, have successfully adapted to be able to grow at high temperatures (35°C) and have a fitness advantage over the parental strain across a range of temperatures.

Evolved isolates have altered colony morphologies and titan cell production

We next asked whether thermal adaptation in our evolved strains was accompanied by alteration of other physical or morphological properties of the fungi. High temperature is a known regulator of different aspects of cryptococcal biology, including pathogenicity-related phenotypes such as capsule production, cell size, and melanization, among others[24]. Close investigation of colony morphology revealed differences in our harvested clonal samples. The parental strain, Ftc239-1, has smooth, small colonies that are cream-white in color. Two of our evolved strains (TA1-1 and TA8-2) exhibited changes in one or more of these features, while the third strain, TA8-3, maintained the parental phenotype. TA1-1 colonies were consistently larger than the parental and took on a mucoid appearance (Figure 2B, Supplementary Table 1). These mucoid colonies have a glossy appearance with smooth edges and form a looser pellet when spun down in liquid culture[25]. TA8-2 maintained the smooth colony phenotype seen in the parental strain, but the colonies were markedly larger (Supplementary Table 2). Interestingly, beyond these three strains, more than half of the other 33 endpoint colonies developed a mucoid colony morphology, which suggests that the mucoid phenotype confers some advantage for surviving thermal stress or that there may be overlap in the genetic pathways that control these two traits (Supplementary Tables 1 and 2).

Given that colony morphology varied across our evolved isolates, we were curious what other aspects of cell morphology might be altered in these strains. In particular, we looked at titan cell formation and capsule production, two aspects of cryptococcal morphology induced by host-like conditions, including high temperature. Titan cells are large (>10 μm), polyploid cells that are induced during *in vivo* infection and can be produced under certain conditions *in vitro*[26]. Larger cell sizes inhibit phagocytosis by immune cells and a polyploid genome allows for more mutational flexibility, both of which allow the yeast to survive and adapt to host conditions during infection. We observed substantial changes in titan cell formation in each of our evolved isolates. TA1-1 produced significantly more titan cells than the parental strain (Figure 3D and E and Supplemental Figure 2A). In contrast, TA8-2 and TA8-3 did not produce any cells large enough to be classified as titan cells suggesting that thermal adaptation in these strains has come at a cost for cell size variation.

The polysaccharide capsule is a defining feature of cryptococcal cells that, similar to titanization, plays an important role during infection. Using *in vitro* protocols to induce capsule production, we observed that while the parental Ftc239-1 strain produces significantly more capsule than laboratory strains like KN99α, there were no major differences in capsule size across our parental and evolved isolates (Figure 3D and F, and Supplemental Figure 2B). So, while some infection-relevant traits like titanization, are altered in these thermally adapted isolates, others, like capsule production, remain unchanged by adaptation to high temperature.

Antifungal drug susceptibility is altered in thermally adapted strains

In addition to thermal stress, fungal cells are subjected to a wide range of other stressors both in the environment and during infection, prompting us to ask whether our evolved isolates may also be more resistant to other types of cellular stress. We decided to explore this question using exposure to the antifungal drug fluconazole as a clinically relevant test to investigate the interface between thermal adaptation and other possible stressors. Specifically, we determined the minimum inhibitory concentration (MIC) of fluconazole for each of our isolates at 35°C. While the parental strain had an MIC of about 8 µg/ml, we observed modest changes of the MICs in each of the evolved isolates (Figure 4A). TA1-1 had an increased MIC, between 12 and 16 ug/ml, compared to the parental strain (Figure 4B). In contrast, TA8-2 and TA8-3 were slightly less resistant to fluconazole, with MICs between 4 and 6 ug/ml and 3 and 4 ug/ml, respectively (Figure 4C and D). This suggests that the cross-stress advantages of thermal adaptation may depend on the conditions in which the yeasts evolve, but also that in some scenarios adaptation to higher temperature can lead to a concurrent increase in antifungal resistance.

Evolved isolates have distinct mutations that vary between populations

Given the strong growth advantage of our passaged strains along with the phenotypic differences across these isolates, we hypothesized that they likely carried adaptive genetic lesions that underlie their phenotypes. To assess the genetic basis of adaptation in our three thermally-adapted isolates, we performed whole genome sequencing of both our parental isolate and the clonal samples (TA1-1, TA8-2, and TA8-3).

We observed unique mutations across both colonies from the same population (TA8-2 and TA8-3) and across populations (YPD vs YNB, TA1-1 vs TA8-2/-3). In the YPD-passaged TA1-1, we identified four fixed mutations affecting a range of different genes and with varying effects, from intronic mutations to frameshifting insertions (Table 1). Intriguingly, one of the mutations we identified is a nonsense mutation in the *PBS2* gene. Pbs2 is a member of the HOG pathway, which regulates cellular stress responses in *C. neoformans* and other related species, including response to high temperature stress[27].

In the two isolates derived from our TA8 YNB-evolved population, TA8-2 and TA8-3, we found six mutations that were shared across both isolates and were also present in a pooled population culture indicating they were fixed in the TA8 population (Table 2). Again, the identified mutations had a range of predicted effects on protein function, though several mutations were particularly interesting in light of some of our other data. In particular, we identified a frameshift mutation in the gene *SSK2*, which, along with *PBS2*, is another integral component of the HOG pathway[28]. The fact that we recovered mutations in two key HOG-pathway genes in these independently evolved populations highlights the importance of this pathway in responding to environmental stress, although the exact impact of these mutations on cryptococcal cell biology remains to be seen.

We also recovered a single nucleotide deletion resulting in a frameshift in the gene *LMP1* in the YNB-evolved TA8 population. *LMP1* has previously been shown to be required for the production of titan cells in *C. neoformans*[29,30]. All of the tested strains carrying this mutation from the TA8 population were defective in our titan cell formation experiments, suggesting that

286 this frameshift mutation likely results in a loss of Lmp1 function (Figure 3D and E). Whether this
287 mutation in *LMP1* also contributes to the ability of these strains to grow at high temperatures is
288 still an open question.
289 In addition to the six mutations that were shared across the clonal isolates from the
290 YNB-evolved TA8 population, we also identified several additional mutations that were present
291 in TA8-3, but not in TA8-2 (Table 3). This suggests, like our phenotypic assays, that population
292 heterogeneity exists at the end of these thermal adaptation experiments. How these mutations
293 were acquired during the course of evolution along with their impact on thermotolerance in
294 these strains are an important avenue of future study. Nevertheless, these data suggest that
295 adaptation of this environmental strain of *C. neoformans* to high temperature may occur through
296 alteration of multiple genetic pathways and varies across populations and nutrient conditions.
297
298 **Discussion**
299 Understanding how environmentally derived pathogenic microbes adapt to different
300 environments, such as increasing temperatures, and the impacts this will have on disease
301 incidence and severity are of critical importance as climate change advances. In this study, we
302 employed experimental evolution to investigate the ability of *Cryptococcus neoformans*, an
303 important human fungal pathogen, to adapt to a high temperature environment and how this
304 alters consequential phenotypes.
305 We used an environmentally isolated *C. neoformans* strain, Ftc239-1, which exhibited
306 attenuated growth under normal laboratory culture conditions (30°C) and severe growth defects
307 at human body temperature (37°C). During serial passaging at increasing temperatures,
308 however, this strain was able to rapidly adapt, gaining the ability to grow better at high
309 temperature (≥35°C) than the parental strain over a very short timespan. While this increased
310 growth ability could suggest an adaptation to the media rather than the temperature, our spot
311 assay data suggests otherwise, as the evolved strains grew better on both YPD and YNB at
312 35°C than the parental strain (Figure 2B and C). Our results also show that the growth
313 advantage of our evolved strains was even more pronounced at 37°C, which was outside the
314 range of temperatures used during serial passaging. This suggests that adaptation to modest
315 temperature increases may affect growth at high temperatures more broadly. But how far does
316 this growth advantage extend?
317 Probing whether there is an upper temperature limit to the fitness advantage in these thermally
318 adapted strains is an interesting and important line of inquiry, especially in light of the genetic
319 mutations we identified. Two of the mutations that became fixed in our populations seem to be
320 loss of function alleles of genes in the HOG pathway, which is responsible for environmental
321 stress responses. Previous work has suggested that mutations in this pathway result in
322 tradeoffs for growth advantages over 40°C[27,28]; therefore future work must be done to reveal
323 what the upper thermal limit may be for the evolved isolates we recovered in this study.
324 While the evolved isolates have a clear fitness advantage at high temperature, changes
325 in cell morphology hint at how these evolved cryptococcal strains may be coping with the
326 increased thermal stress. In particular, we noted both changes in colony morphology but also in
327 the ability of cells from our evolved populations to alter cell size (Figure 3 and Supplemental
328 Figure 1). Our evolved TA1-1 isolate has significantly increased titan cell formation, which could
329 give it an advantage in *in vivo* infection due to the polyploidization and increased genome
330 flexibility that accompany titan cell formation and may allow for easier adaptation to host
331 conditions (Figure 3D and E). However, increased titanization rates were not universal features
332 of the evolved isolates recovered in our experiment. The two strains we analyzed from a YNB-
333 evolved population, TA8-2 an TA8-3, lack the ability to produce titan cells altogether and we also
334 noted changes in other features of many of our evolved isolates, such as mucoidy, which varied
335 both across nutrient conditions and populations (Figure 3D and E and Supplemental Figure 1).
336 The diverse effects of our adaptation experiment on titan cell formation and other cellular

features across adapted isolates may shed light on the effect of nutrient conditions during adaptation and also highlight the heterogeneity of our populations after passaging, suggesting that there may be many adaptive strategies for thermotolerance in this species.

Another critical question with clinical relevance that stems from this work is whether adaptation to one form of stress (i.e. temperature) confers resistance to other forms of stress (i.e. antifungal drug treatment). Previous work has demonstrated that strains with increased titanization rates have enhanced resistance to antifungal drugs suggesting that these diverse phenotypes have wide-ranging impacts on cryptococcal biology[31]. Interestingly, our data directly corroborates the connection between titanization and antifungal resistance, while also providing a link to thermal adaptation. TA1-1, which has increased titan cell production, is more resistant to fluconazole than the parental strain. TA8-2 and TA8-3, which do not produce titan cells at all, have lower fluconazole MICs than the parental strain (Figure 4). Our data characterizing TA1-1 and antifungal drug resistance is particularly compelling, as it suggests that rising environmental temperatures may not only impact the prevalence of species capable of establishing human infection, but may also affect the treatment strategies for such infections. However, given the evidence from TA8-2 and TA8-3, this cross-stress fitness advantage may depend on specific nutrient conditions, further underscoring the importance of studies examining the interplay between nutrients, cell size, stress resistance, and thermal adaptation.

In the two sequenced populations from our evolution, we identified multiple, non-overlapping genetic lesions which we hypothesize give rise to the phenotypes we observe in our evolved isolates. The HOG pathway, a regulator of environmental stress responses, was the target of two of these mutations, in two separate populations, resulting in a presumed loss of function of the proteins Pbs2 and Ssk2 (Tables 1 and 2)[27,28]. This convergence on the HOG pathway in independent populations suggests it is an integral part of cryptococcal thermal adaptation. Beyond the HOG pathway, mutations in our evolved isolates varied widely. Other mutations that were identified in the strains sequenced here were intronic, intergenic, in retrotransposons, and/or in uncharacterized proteins, and as such, have less predictable effects on gene function and the adaptive phenotypes we observed (Tables 1, 2, and 3). The diversity of mutations and pathways sampled in just two of our eight adapted populations further supports the hypothesis that there may be many routes by which this species can evolve thermotolerance. Therefore, our investigation offers an exciting avenue to discover new biology in regard to these mutations and their role in thermal adaptation.

Our work here begins a foray into the study of how our changing world will alter the pathogens that infect us. As our findings suggest, host body temperature may not represent as severe a barrier to *C. neoformans* and other fungal infections as environmental temperatures increase. This work, therefore, provides a vital foundation to illuminate the consequences a changing world will have for the health of future generations.

Materials and Methods

Strains and growth conditions

All strains were stored long term at -80°C in growth media—either yeast extract peptone dextrose (YPD) or yeast nitrogen base (YNB)—supplemented with 20% glycerol. Strains were inoculated by streaking out onto YPD plates and incubated for 2-3 days at 30°C before use in experiments. A full list of strains used can be found in Supplemental File 1.

Serial passaging of *C. neoformans* at increasing temperatures

For the first passage, an overnight culture of Ftc239-1 was inoculated from a single colony and grown in YPD with shaking for 16 hours at 30°C. This culture was centrifuged at 3000 x g for 5 minutes and washed twice with autoclaved MilliQ water and resuspended in 5 mL of water before the OD was measured. Cells were normalized to an OD of 0.05 (~4.04×10^6 cells/ml) in 5 mL of either YPD or YNB with 2% added glucose (4 replicate cultures of each).

388 The remaining starting inoculum culture was mixed 1:1 with 40% glycerol and aliquots were
389 frozen at -80°C.
390 The cultures were incubated at 30°C with shaking at 225 rpm for 48 hours. After 48
391 hours, the OD of each individual culture was measured and re-diluted to an OD of 0.05 in 5 mL
392 of the appropriate growth media. Passaging proceeded as above from this point. The
393 temperature was increased once the majority (>75%) of the cultures had reached three to four
394 doublings in the 48 hour culture period. Incubation temperature was increased by 1°C from
395 30°C to 33°C and 0.5°C from 33°C to 35°C. Aliquots from each individual culture were frozen
396 down as above at the start and end of each temperature, as well as every other passage.
397 Following the final passage at 35°C, multiple aliquots were frozen. Samples from each
398 population were also serially diluted and plated onto YPD plates for CFU determination.
399 Individual colonies from these plates were picked into 5 mL of YPD, grown overnight, and frozen
400 for use in phenotyping experiments (Figure 2A).
401 Though the experimental passaging was carried out based on OD measurements, the
402 actual amount of yeast passaged may not have been adequately reflected by the OD. In the
403 course of our characterization of experimentally evolved strains, we determined that some of the
404 populations were contaminated with *Staphylococcus hominis*, which absorbs at the same OD
405 and likely means that passage bottlenecks were more severe than intended. However, this
406 contamination did not affect our ability to isolate thermally adapted fungal clones. Further, our
407 data suggest that the bacterial contaminant has not significantly impacted the thermal
408 adaptation of the *Cryptococcus*.
409
410 **Yeast spot assays**
411 *C. neoformans* strains of interest were grown overnight in YPD at 30°C. The cultures
412 were then centrifuged at 3000 x g for 5 minutes, washed twice with autoclaved MilliQ water, and
413 resuspended in 5 mL of MilliQ water. The OD_{600} of each culture was measured, and the OD was
414 adjusted to OD 1. 10-fold serial dilutions of each culture were then made down to OD 0.0001.
415 2.5 ul of each dilution was spotted onto YPD and YNB plates, and the plates were incubated at
416 the desired temperature for a total of 72 hours. Plates were imaged on Gel Doc XR+ (BioRad)
417 after 48 and 72 hours.
418
419 **Strain construction and molecular biology**
420 All genetic manipulations were done using CRISPR-mediated gene editing and the
421 TRACE system following previously published protocols[32,33]. Briefly, gRNAs were generated
422 using guide-specific primer and amplification from pBHM2329 plasmid. *CAS9* was amplified for
423 transformation from the pBHM2403 plasmid.
424 For insertion of the hygromycin B cassette as the Safe Haven 2 locus (SH2), we used a
425 VNB lineage-specific guide targeting this locus. A repair template plasmid carrying the ~1 kb of
426 sequence immediately 5' and 3' to this gRNA sequence from the H99 genome was constructed
427 using HiFi DNA Master Mix (NEB Cat#E2621) with a standard HYG^R cassette inserted between
428 the two flanks. Repair templates were then PCR amplified from this plasmid for CRISPR
429 transformations. DNA concentrations in CRISPR transformations were as follows: 250 ng Cas9,
430 100 ng gRNA, and 2.5 µg repair template.
431
432 **Transformant selection and genotyping**
433 Following electroporation of CRISPR reagents, strains were plated onto selective media
434 (YPAD+HYG) and allowed to grow for 2-3 days at 30C. Individual colonies were then patched
435 onto non-selective YPD media for 2-3 passages before being patched back onto selective
436 media to identify stable genomic integrants.
437 Colonies were genotyped by colony PCR following previously published protocols[34].
438 Genomic sequences were amplified from gDNA extracted from candidate colonies and

integration of the drug cassette at the SH2 locus was confirmed by Sanger sequencing. PCRs were also performed to ensure that no strains had integrated the gRNA or *CAS9* constructs. All primer sequences for generating CRISPR reagents and genotyping mutants have been previously published[34].

Competition assays

For competition experiments, *C. neoformans* strains of interest were grown at 30°C overnight in YPD. For experiments done in YPD, the OD was measured for each test strain and for a parental Ftc239-1 strain carrying a HYG-resistance cassette at the SH2 locus. Cell suspensions at a concentration of ~4.04 x 10^6 cells/mL were made for each individual strain. Cell suspensions were mixed 1:1 (test strain : labeled parental) in a total of 40 mL YPD media before adding 5 mL to individual culture tubes. Each competition was performed in biological triplicate for each temperature (30°C or 35°C). CFUs for the initial mixtures were determined by serially diluting the suspensions and plating onto both YPD and YPAD+HYG plates. Competition cultures were grown for 24 hours at 225 rpm at their respective temperatures. After 24 hours, serial dilutions were plated onto nonselective and selective media plates as above. Competitive Index here is calculated as: $Competitive\ Index = \frac{\frac{24\ hr\ CFU\ Test\ Strain}{24\ hr\ CFU\ HYG\ Control}}{\frac{0\ hr\ CFU\ Test\ Strain}{0\ hr\ CFU\ HYG\ Control}}$

For experiments done in YNB, overnight YPD cultures were washed twice and resuspended in 5 mL of MilliQ water before setting up the experiment as above.

Fluconazole MIC determinations

Overnight cultures of *C. neoformans* strains were adjusted to a density of ~5 x 10^6 cells/mL and were spread onto either YPD-agar or RPMI-agar medium with L-glutamine and without sodium bicarbonate. Fluconazole Etest strips (bioMérieux) were placed on the agar surface of one of the replicate plates once the cultures had dried. Plates were incubated at either 30°C or at 35°C, and imaged after 72 and 96 hours. Only strains with robust growth on control YPD plates were imaged and used to determine MIC values.

Titan cell induction and capsule assays

Titan cell induction was performed following previously published protocols[35]. Briefly, strains were cultured overnight in YPD at 30°C. Cultures were centrifuged at 3000 x g for 5 minutes, washed three times in PBS, and resuspended in 3 mL of PBS. The cells were diluted to ~5 x 10^3 cells/ml in 4 ml of serum-free RPMI 1640 media. One milliliter of each strain dilution was plated into three replicate wells of a 24-well plate. The plate was incubated at 37C with 5% CO_2 without shaking for 7 days. Cells were then fixed with formaldehyde, stained 1:1 with India Ink, and imaged on a Zeiss Axio Observer 7 microscope at 100x.

Capsule was induced following previously published protocols[36]. *C. neoformans* strains of interest were grown overnight (16-18 hours) in YPD at 30°C. Cultures were centrifuged, washed twice with PBS, and resuspended in 5 mL of PBS. OD_{600} was measured for each strain, and the strains were subcultured to an OD of 0.3 in 4 mL of DMEM media containing 10% FBS, non-essential amino acids, and penicillin/streptomycin. Two milliliter aliquots of each dilution were incubated in a 6-well plate at 37°C with 5% CO_2. After 48 hours of incubation, the cells were fixed and imaged as above.

For both capsule and titan inductions, cell size measurements for each strain were made for 50 cells under each condition using the QCA MatLab program[37]. Capsule thickness here was calculated as: capsule thickness = (total diameter – cell body diameter)/2.

Genomic DNA extraction and sequencing

Single colonies or pooled culture stocks were inoculated into 50 mL of YPD and grown overnight, or until the culture was fully saturated, with shaking at 30C. Cells were collected by centrifugation and lyophilized overnight. High-molecular-weight genomic DNA was isolated following the CTAB protocol. Following CTAB extraction, samples were further purified using the ProNex Size-Selective Purification System (Promega). Concentrations were measured by Qubit dsDNA broad range assay. For Nanopore sequencing of Ftc239-1, one microgram of HMW gDNA was prepared for sequencing using the SQK_LSK110 Kit and run on an R9 (FLO-MIN106) flow cell. For Illumina sequencing, samples were sheared with a Covaris S2 Focused-ultrasonicator and libraries were prepared using the New England Biolabs NEBNext Ultra II DNA Library Prep kit (cat#E7634L) with an average insert size of 450 bp. Ten strains were barcoded and pooled, and 150x150 bp paired-end reads were collected on a NovaSeq S4 Flow Cell with the v1.5 Reagent Kit. Illumina library preparation and sequencing was performed by the University of Utah's High Throughput Genomics core facility at the Huntsman Cancer Institute. Raw sequencing datasets are available through the SRA under the BioProject Accession PRJNA1096649.

Sequencing analysis

A chromosome scale assembly of the parental Ftc239-1 strain was drafted largely as previously published[34]. Briefly, fast5 files from Nanopore sequencing were re-basecalled using guppy-gpu (v6.4.2) and the resulting fastq files were assembled using Canu (v 2.1.1) with an estimated genome size of 20 megabases and default settings[38]. The Canu assembly had 14 chromosome-scale contigs. Shorter contigs mapping to the mitochondrial genome or repetitive genomic regions were manually trimmed. This assembly was polished once with Nanopore reads using Medaka (1.7.2; https://github.com/nanoporetech/medaka) and then polished and additional five times with Illumina reads from the parental strain using pilon (v1.24)[39]. The mitochondrial genome was assembled from Illumina reads using GetOrganelle (v1.7.5.3) with the fungus_mt setting and confirmed by comparison to the trimmed contigs assembled by Canu[40]. This mitochondrial genome was manually added to the assembly. Chromosomes were named based on comparison to other reference assemblies. The complete draft assembly was annotated *de novo* using funannotate (v1.8.15) and publicly available RNA-seq datasets of *C. neoformans* strains grown under a variety of conditions (SRA Accession Numbers: SRR646263, SRR639772, SRR646268, SRR646265)[41]. *De novo* annotations were functionally annotated by BLAST to the reference (H99) proteome available from Uniprot and annotation files were updated using AGAT (v1.0.0)[42].

For Illumina sequencing data of isolates from the end of the evolution, adapters were trimmed using Trimmomatic (v0.39) and reads were aligned to our *de novo* assembly using bwa-mem2 (v 2.2.1)[43,44]. Duplicates were marked and read groups added with Picard and the resulting files were sorted and indexed with SAMtools[45]. Variants were called using sorted BAM files with FreeBayes (v0.9.21.7) with the following options: -p 1 --min-alternate-fraction 0.8 --standard-filters[46]. The predicted impacts of called variants were assessed using SnpEff using our *de novo* assembly as reference[47]. Called variants were also cross-checked by analysis with breseq (v0.37.1) with settings altered to reject indels and variants predicted in regions of long homopolymer runs (options: --consensus-reject-indel-homopolymer-length 3 --consensus-reject-surrounding-homopolymer-length 3)[48]. All sequencing analysis was performed using resources through the University of Utah Center for High Performance Computing.

Acknowledgements

We thank John Perfect for providing the environmental isolates used in this study. This work was funded by a Helen Hay Whitney Foundation postdoctoral fellowship to Z.A.H., a Burroughs Wellcome Fund Investigator in the Pathogenesis of Infectious Disease award to N.C.E., and an NIH R35 (R35GM1 34936) awarded to N.C.E.

538
539 **Author Contributions**
540 Conceptualization: M.J.W.S., Z.A.H.
541 Methodology: M.J.W.S., Z.A.H.
542 Software: Z.A.H.
543 Validation: M.J.W.S., Z.A.H.
544 Formal Analysis: M.J.W.S., Z.A.H.
545 Investigation: M.J.W.S., Z.A.H.
546 Data Curation: M.J.W.S., Z.A.H.
547 Writing-Original Draft: M.J.W.S., Z.A.H.
548 Writing-Review and Editing: M.J.W.S., Z.A.H., N.C.E.
549 Visualization: M.J.W.S., Z.A.H.
550 Supervision: Z.A.H., N.C.E.
551 Funding acquisition: N.C.E.
552
553 **Competing Interests**
554 The authors declare no competing financial interests.
555
556 **Figure Legends**
557
558 **Figure 1. Phenotypic variation of *C. neoformans* environmental isolate growth at high**
559 **temperatures. (**A) Phylogenetic tree of *C. neoformans* strains used in this study adapted from
560 Desjardins *et. al*. The primary strain used in subsequent figures, Ftc239-1, is indicated in bold
561 and boxed. (B and C) Growth of *C. neoformans* strains on YNB (B) or YPD (C) agar plates at
562 30°C (left) or 37°C (right).
563
564 **Figure 2. Serial passaging of *C. neoformans* selects for strains with increased**
565 **thermotolerance.** (A) Schematic of the serial passaging set-up used in this study. See also
566 Materials and Methods. Populations TA1-TA4 were passaged in YPD; TA5-TA8 were passaged
567 in YNB. (B and C) Growth of serially passaged isolates on YPD (B) or YNB (C) agar plates.
568 Strains were tested for growth at temperatures they experienced during the experimental
569 evolution passaging (30 and 35°C, middle panels). Growth was also assessed at temperatures
570 outside of the range used during passaging (26°C and 37°C, outer panels).
571
572 **Figure 3. Thermally-adapted isolates outcompete the parental strain at high temperature**
573 **and display additional phenotypic changes.** (A) Schematic of the competition experiment
574 set-up between the HYG^R-labeled parental strain and serially-passaged isolates at 30°C or
575 35°C. See also Materials and Methods. (B and C) Competition experiments between HYG^R-
576 labeled parental and unlabeled parental (blue), TA1-1 (dark red), TA8-2 (orange), and TA8-3
577 (light orange) strains in either YPD (B) or YNB (C) at both 30°C and 35°C. Competitive indices
578 (CIs) are calculated as indicated in Methods. A CI=1 (dotted line) indicates equal growth of the
579 two strains. Plotted values indicate the average value ± SEM of three replicate experiments
580 carried out on three separate days; dots indicate the average value of biological replicates from
581 a single experiment. (D) Representative images from cells in titan-inducing (left) and capsule-
582 inducing (right) conditions for parental and evolved strains. Images from different conditions are
583 at the same scale with all scale bars representing 10 μm. (E) Measurements of cell body
584 diameter from cells grown under titan inducing conditions. Percentages above each strain
585 indicate the percent of cells with a diameter >10 μm (dotted line). Error bars show mean ± SD
586 for one representative experiment. (F) Measurements of capsule thickness from cells grown
587 under capsule inducing conditions. Capsule thicknesses were calculated as indicated in
588 Materials and Methods. Median and quartiles are indicated with dashed lines for cells from one

589 representative experiment. For (E) and (F), 50 cells were measured per strain. Significance was
590 assessed in comparison to the parental Ftc239-1 strain by ordinary one-way ANOVA with
591 Dunnett's multiple comparisons test.
592
593 **Figure 4. Thermal adaptation alters antifungal drug susceptibility in serially-passaged**
594 **isolates.** Fluconazole minimum inhibitory concentrations (MICs) for the parental (A) and
595 evolved (B-D) isolates on RPMI agar plates with E-test strips.
596
597 **Table 1. Fixed mutations in the TA1-1 YPD-passaged strain.**
598
599 **Table 2. Fixed mutations in the TA8 YNB-passaged population.** These mutations are
600 present in all of the sequenced TA8 clonal isolates.
601
602 **Table 3. Additional fixed mutations in TA8-derived strains.** These mutations are only
603 present in the indicated colony from the TA8 population.
604

References

1. *Climate Change 2022: Impacts, Adaptation, and Vulnerability - Summary for Policymakers*. https://www.ipcc.ch/report/ar6/wg2/chapter/summary-for-policymakers/ (2022).
2. Garcia-Solache, M. A. & Casadevall, A. Global Warming Will Bring New Fungal Diseases for Mammals. *MBio* **1**, e00061-10 (2010).
3. Robert, V. A. & Casadevall, A. Vertebrate Endothermy Restricts Most Fungi as Potential Pathogens. *J. Infect. Dis.* **200**, 1623–1626 (2009).
4. Gorris, M. E., Treseder, K. K., Zender, C. S. & Randerson, J. T. Expansion of Coccidioidomycosis Endemic Regions in the United States in Response to Climate Change. *GeoHealth* **3**, 308–327 (2019).
5. Cogliati, M. Global warming impact on the expansion of fundamental niche of Cryptococcus gattii VGI in Europe. *Environ. Microbiol. Rep.* **13**, 375–383 (2021).
6. Casadevall, A., Kontoyiannis, D. P. & Robert, V. Environmental Candida auris and the Global Warming Emergence Hypothesis. *MBio* **12**, e00360-21 (2021).
7. Cavicchioli, R. *et al.* Scientists' warning to humanity: microorganisms and climate change. *Nat. Rev. Microbiol.* **17**, 569–586 (2019).
8. Nnadi, N. E. & Carter, D. A. Climate change and the emergence of fungal pathogens. *PLoS Pathog.* **17**, e1009503 (2021).
9. Idnurm, A. *et al.* Deciphering the Model Pathogenic Fungus Cryptococcus Neoformans. *Nat. Rev. Microbiol.* **3**, 753–764 (2005).
10. Rajasingham, R. *et al.* The global burden of HIV-associated cryptococcal infection in adults in 2020: a modelling analysis. *Lancet Infect. Dis.* **22**, 1748–1755 (2022).
11. Rhodes, J. *et al.* Tracing Genetic Exchange and Biogeography of Cryptococcus neoformans var. grubii at the Global Population Level. *Genetics* **207**, 327–346 (2017).
12. Mitchell, T. G., Castañeda, E., Nielsen, K., Wanke, B. & Lazéra, M. S. Environmental Niches for Cryptococcus neoformans and Cryptococcus gattii. in *Cryptococcus* 235–259 (John Wiley & Sons, Ltd, 2010).
13. Desjardins, C. A. *et al.* Population genomics and the evolution of virulence in the fungal pathogen Cryptococcus neoformans. *Genome Res.* **27**, 1207–1219 (2017).
14. Chen, Y. *et al.* Comparative analyses of clinical and environmental populations of Cryptococcus neoformans in Botswana. *Mol. Ecol.* **24**, 3559–3571 (2015).
15. Litvintseva, A. P. *et al.* Evidence that the human pathogenic fungus Cryptococcus neoformans var. grubii may have evolved in Africa. *PLoS One* **6**, e19688 (2011).
16. Brown, S. M., Campbell, L. T. & Lodge, J. K. Cryptococcus neoformans, a fungus under stress. *Curr. Opin. Microbiol.* **10**, 320–325 (2007).
17. Glazier, V. E. & Panepinto, J. C. The ER stress response and host temperature adaptation in the human fungal pathogen Cryptococcus neoformans. *Virulence* **5**, 351–356 (2014).
18. Leach, M. D. & Cowen, L. E. Surviving the Heat of the Moment: A Fungal Pathogens Perspective. *PLoS Pathog.* **9**, e1003163 (2013).
19. Stempinski, P. R. *et al.* Genetic contribution to high temperature tolerance in Cryptococcus neoformans. *Genetics* **217**, iyaa009 (2021).
20. Bennett, A. F. & Lenski, R. E. Evolutionary Adaptation to Temperature II. Thermal Niches of Experimental Lines of Escherichia coli. *Evolution* **47**, 1–12 (1993).
21. Garcia-Rios, E. *et al.* Thermo-adaptive Evolution to Generate Improved Saccharomyces cerevisiae Strains for Cocoa Pulp Fermentations. *Int. J. Food Microbiol.* **342**, 109077 (2021).
22. Huang, C.-J., Lu, M.-Y., Chang, Y.-W. & Li, W.-H. Experimental Evolution of Yeast for High-Temperature Tolerance. *Mol. Biol. Evol.* **35**, 1823–1839 (2018).

655 23. Longan, E. R. & Fay, J. C. Experimental evolution of Saccharomyces uvarum at high
656 temperature yields elevation of maximal growth temperature and loss of the mitochondrial
657 genome. *microPublication Biology* (2023) doi:10.17912/micropub.biology.000831.
658 24. Montoya, M. C., Magwene, P. M. & Perfect, J. R. Associations between Cryptococcus
659 Genotypes, Phenotypes, and Clinical Parameters of Human Disease: A Review. *Journal of*
660 *Fungi* **7**, 260 (2021).
661 25. Guerrero, A., Jain, N., Goldman, D. L. & Fries, B. C. Phenotypic switching in Cryptococcus
662 neoformans. *Microbiology* **152**, 3–9 (2006).
663 26. Dambuza, I. M. *et al.* The Cryptococcus neoformans Titan cell is an inducible and regulated
664 morphotype underlying pathogenesis. *PLoS Pathog.* **14**, e1006978 (2018).
665 27. Bahn, Y.-S. & Jung, K.-W. Stress Signaling Pathways for the Pathogenicity of
666 Cryptococcus. *Eukaryot. Cell* **12**, (2013).
667 28. Bahn, Y.-S., Geunes-Boyer, S. & Heitman, J. Ssk2 Mitogen-Activated Protein Kinase
668 Kinase Kinase Governs Divergent Patterns of the Stress-Activated Hog1 Signaling Pathway
669 in Cryptococcus neoformans. *Eukaryot. Cell* **6**, 2278–2289 (2007).
670 29. Hommel, B. *et al.* Titan cells formation in Cryptococcus neoformans is finely tuned by
671 environmental conditions and modulated by positive and negative genetic regulators. *PLoS*
672 *Pathog.* **14**, e1006982 (2018).
673 30. Janbon, G. *et al.* Analysis of the Genome and Transcriptome of Cryptococcus neoformans
674 var. grubii Reveals Complex RNA Expression and Microevolution Leading to Virulence
675 Attenuation. *PLoS Genet.* **10**, e1004261 (2014).
676 31. Zhou, X. & Ballou, E. R. The Cryptococcus neoformans Titan Cell: From In Vivo
677 Phenomenon to In Vitro Model. *Current Clinical Microbiology Reports* **5**, 252–260 (2018).
678 32. Fan, Y. & Lin, X. Multiple Applications of a Transient CRISPR-Cas9 Coupled with
679 Electroporation (TRACE) System in the Cryptococcus neoformans Species Complex.
680 *Genetics* **208**, 1357–1372 (2018).
681 33. Huang, M. Y. *et al.* Short homology-directed repair using optimized Cas9 in the pathogen
682 Cryptococcus neoformans enables rapid gene deletion and tagging. *Genetics* **220**, iyab180
683 (2021).
684 34. Hilbert, Z. A. *et al.* Distinct pathways of adaptive evolution in Cryptococcus neoformans
685 reveal a mutation in adenylyl cyclase with trade-offs for pathogenicity. *Curr. Biol.* **33**, 4136-
686 4149.e9 (2023).
687 35. Saidykhan, L. *et al.* An in vitro method for inducing titan cells reveals novel features of
688 yeast-to-titan switching in the human fungal pathogen Cryptococcus gattii. *PLoS Pathog.*
689 **18**, e1010321 (2022).
690 36. Zaragoza, O. & Casadevall, A. Experimental modulation of capsule size in Cryptococcus
691 neoformans. *Biol. Proced. Online* **6**, 10–15 (2004).
692 37. Dragotakes, Q. & Casadevall, A. Automated Measurement of Cryptococcal Species
693 Polysaccharide Capsule and Cell Body. *J. Vis. Exp.* 56957 (2018) doi:10.3791/56957.
694 38. Koren, S. *et al.* Canu: scalable and accurate long-read assembly via adaptive k-mer
695 weighting and repeat separation. *Genome Res.* **27**, 722–736 (2017).
696 39. Walker, B. J. *et al.* Pilon: an integrated tool for comprehensive microbial variant detection
697 and genome assembly improvement. *PLoS One* **9**, e112963 (2014).
698 40. Jin, J.-J. *et al.* GetOrganelle: a fast and versatile toolkit for accurate de novo assembly of
699 organelle genomes. *Genome Biol.* **21**, 241 (2020).
700 41. Funannotate documentation — Funannotate 1.8.16 documentation.
701 https://funannotate.readthedocs.io/en/latest/.
702 42. Welcome to AGAT's documentation! — AGAT documentation.
703 https://agat.readthedocs.io/en/latest/.
704 43. Bolger, A. M., Lohse, M. & Usadel, B. Trimmomatic: a flexible trimmer for Illumina sequence
705 data. *Bioinformatics* **30**, 2114–2120 (2014).

44. Vasimuddin, M., Misra, S., Li, H. & Aluru, S. Efficient Architecture-Aware Acceleration of BWA-MEM for Multicore Systems. in *2019 IEEE International Parallel and Distributed Processing Symposium (IPDPS)* 314–324 (IEEE, 2019). doi:10.1109/IPDPS.2019.00041.
45. Danecek, P. *et al.* Twelve years of SAMtools and BCFtools. *Gigascience* **10**, (2021).
46. Garrison, E. & Marth, G. Haplotype-based variant detection from short-read sequencing. *arXiv [q-bio.GN]* (2012).
47. Cingolani, P. *et al.* A program for annotating and predicting the effects of single nucleotide polymorphisms, SnpEff: SNPs in the genome of Drosophila melanogaster strain w1118; iso-2; iso-3. *Fly* **6**, 80–92 (2012).
48. Deatherage, D. E. & Barrick, J. E. Identification of mutations in laboratory-evolved microbes from next-generation sequencing data using breseq. *Methods Mol. Biol.* **1151**, 165–188 (2014).

Supplemental Figures

Supplemental Figure 1. Phenotypic variation of *C. neoformans* parental and evolved isolates. (A and B) Growth of *C. neoformans* parental strain and YPD (A) and YNB (B) evolved isolates on YPD (left) or YNB (right) agar plates at 30 and 35°C.

Supplemental Figure 2. Parental Ftc239-1 displays increases in titan cell formation and capsule production compared to laboratory reference strains. (A) Measurements of laboratory reference (shades of gray) and Ftc239-1 parental (blue) strains cell body diameters from cells grown under titan inducing conditions. Percentages above each strain indicate the percent of cells with a diameter >10 µm (dotted line). Error bars show mean ± SD. (B) Measurements of capsule thickness from cells grown under capsule inducing conditions for laboratory reference (shades of gray) and parental (blue) strains. Median and quartiles indicated by dashed lines. For both panels, 50 cells were measured per strain from one representative experiment. Significance was assessed in comparison to the parental Ftc239-1 strain by ordinary one-way ANOVA with Dunnett's multiple comparisons test. Parental Ftc239-1 measurements in this figure are identical to those found in Figure 3E and F as these strains were all tested as part of a single experiment.

Supplementary Table 1. Colony phenotypes of individual colony isolates of the YPD-passaged populations (TA1-TA4). Isolates discussed in this study are indicated by darkened background.

Supplementary Table 2. Colony phenotypes of individual colony isolates of the YNB-passaged populations (TA5-TA8). Isolates discussed in this study are indicated by darkened backgrounds.

Supplemental Files

Supplemental File 1. List of strains used in this study.

Figure 1

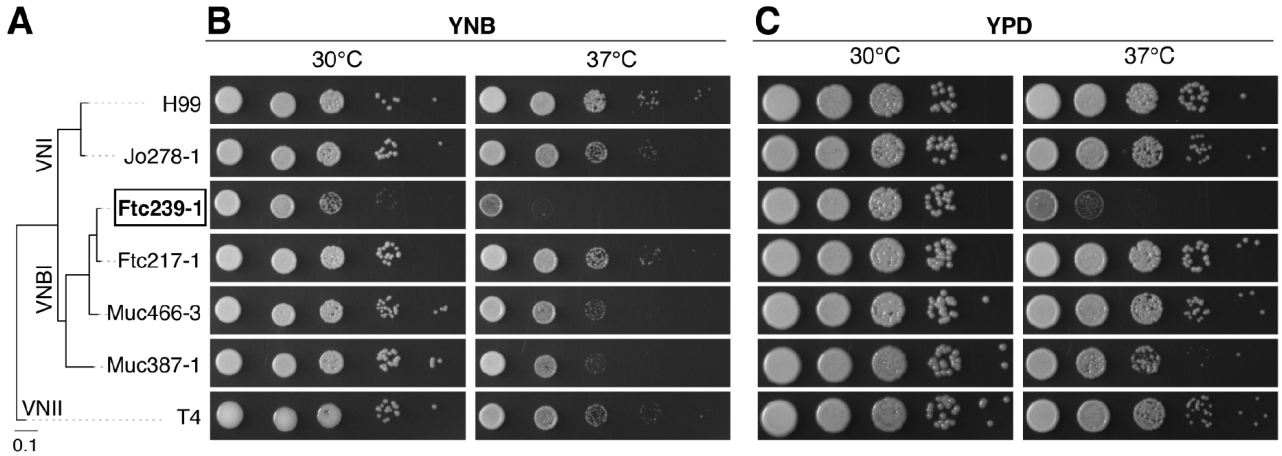
A
B
YNB
30°C
37°C
C
YPD
30°C
37°C
H99
Jo278-1
Ftc239-1
Ftc217-1
Muc466-3
Muc387-1
T4
VNI
VNBI
VNII
0.1

Figure 2

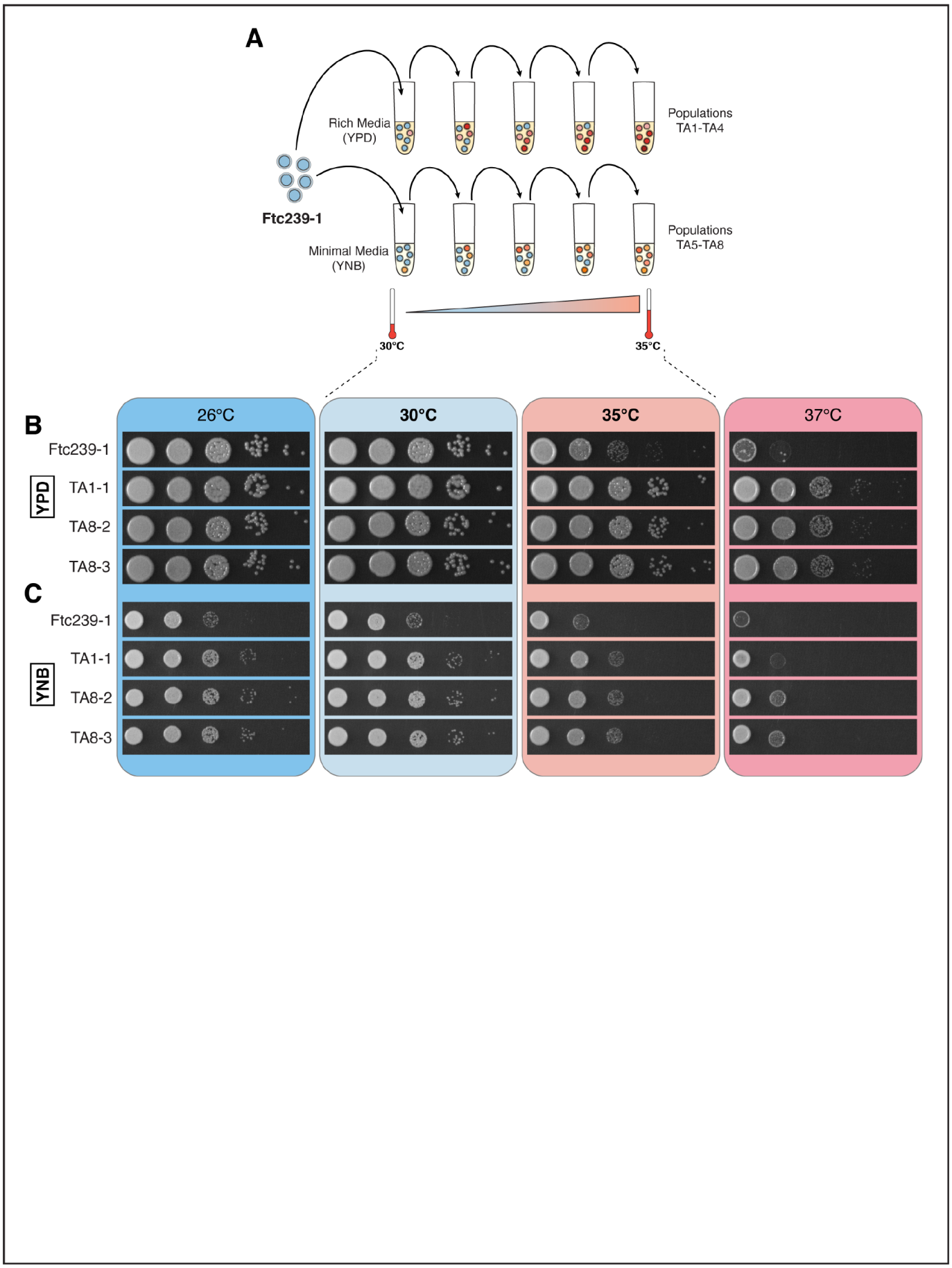
A
Rich Media
(YPD)
Populations
TA1-TA4
Ftc239-1
Minimal Media
(YNB)
Populations
TA5-TA8
30°C
35°C
B
26°C
30°C
35°C
37°C
Ftc239-1
YPD
TA1-1
TA8-2
TA8-3
C
Ftc239-1
YNB
TA1-1
TA8-2
TA8-3

Figure 3

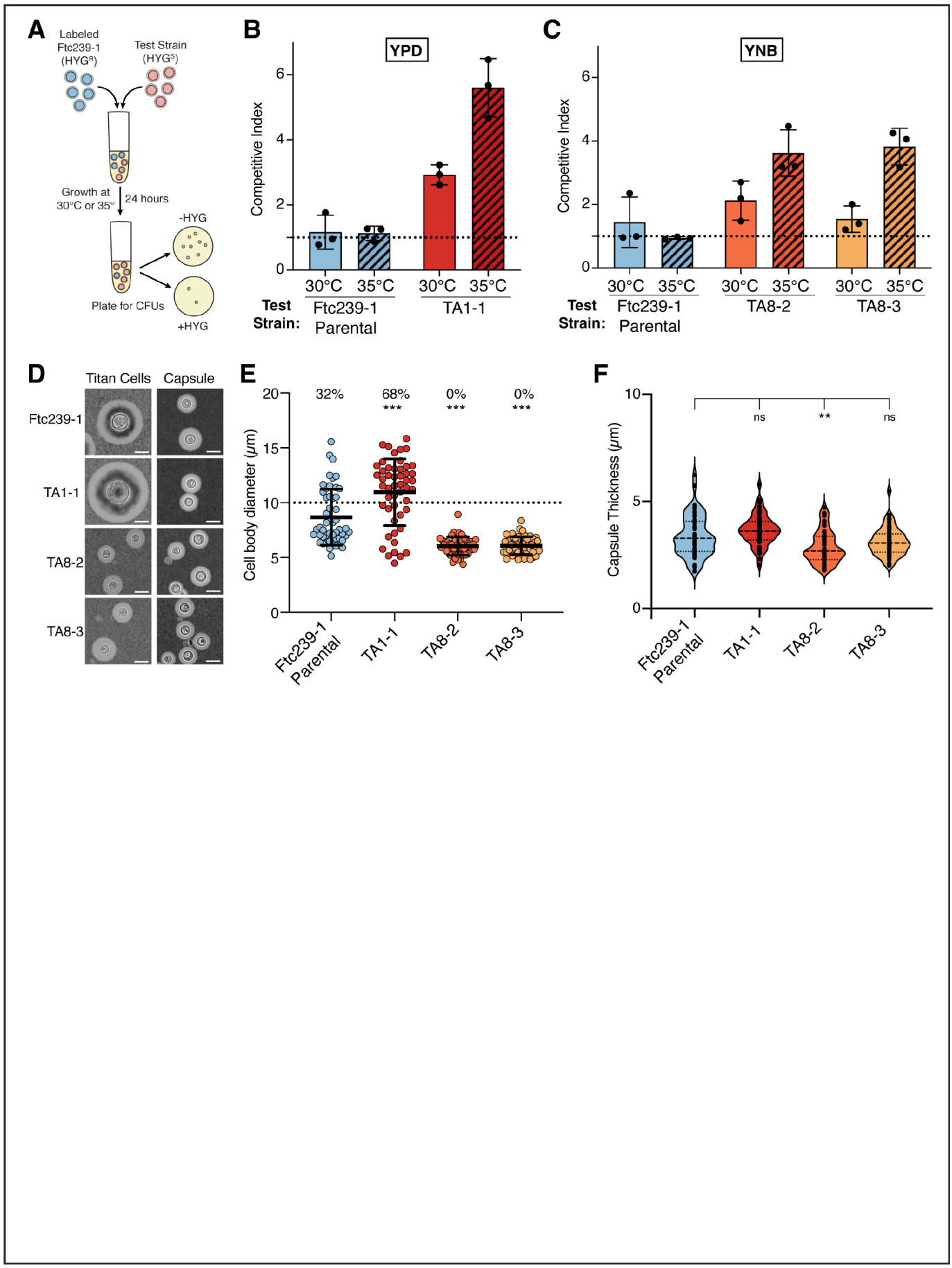
A
Labeled Ftc239-1 (HYG^R)
Test Strain (HYG^S)
Growth at 30°C or 35°
24 hours
-HYG
Plate for CFUs
+HYG
B
YPD
Competitive Index
0
2
4
6
30°C 35°C 30°C 35°C
Test Strain:
Ftc239-1 Parental
TA1-1
C
YNB
Competitive Index
0
2
4
6
30°C 35°C 30°C 35°C 30°C 35°C
Test Strain:
Ftc239-1 Parental
TA8-2
TA8-3
D
Titan Cells
Capsule
Ftc239-1
TA1-1
TA8-2
TA8-3
E
Cell body diameter (μm)
0
5
10
15
20
32%
68%
0%
0%
***
***
***
Ftc239-1 Parental
TA1-1
TA8-2
TA8-3
F
Capsule Thickness (μm)
0
5
10
ns
**
ns
Ftc239-1 Parental
TA1-1
TA8-2
TA8-3

Figure 4

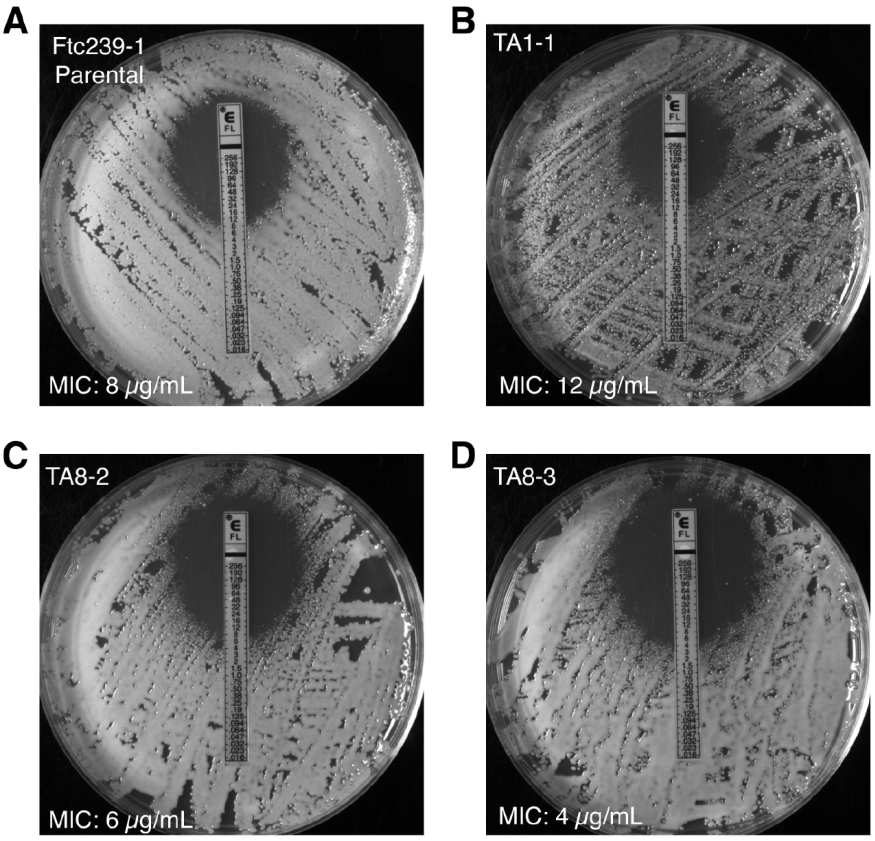
A
Ftc239-1
Parental
MIC: 8 μg/mL
B
TA1-1
MIC: 12 μg/mL
C
TA8-2
MIC: 6 μg/mL
D
TA8-3
MIC: 4 μg/mL

Tables

Table 1

Chr.	Pos.	Gene	Gene Name and Info	Effect	REF	ALT
01	2,000,229	*CNAG_00769*	*PBS2*, HOG pathway MAPKK	Y372*	C	A
02	973,304	*CNAG_03735*	*CAP4*, predicted glycosyltransferase	Intronic	GAAAAAAAAAG	GAAAAAAAAG
06	1,422,809	*CNAG_02028*	predicted serine-arginine protein kinase	G153E	C	T
07	930,986	*CNAG_07655*	hypothetical protein	4 nt Insertion, Frameshift	C	GGGCG

Table 2

Chr.	Pos.	Gene	Gene Name and Info	Effect	REF	ALT
02	1,592,272	*CNAG_06765*	*LMP1*, low mating performance protein	1 nt Deletion, Frameshift	TT	T
04	328,289	*CNAG_05063*	*SSK2*, HOG pathway MAPKKK	1 nt Deletion, Frameshift	TT	T
05	723,192	Intergenic			G	C
08	435,015	*CNAG_03438*	*HXT1*, hexose transporter	G30R	G	C
10	1,058,846	Intergenic *(CNAG_04922 3' UTR)*	*CNAG_04922*, hypothetical protein		C	A
14	928,714	Intergenic	Intergenic		C	T

Table 3

Strain	Chr.	Pos.	Gene	Gene Name and Info	Effect	REF	ALT
TA8-1	07	289,398	Intergenic *(CNAG_05884 5' UTR)*	*KAP123*, predicted importin beta family		CTTTTTTTTTC	CTTTTTTTTC
TA8-3	08	858,513	Intergenic			G	C
TA8-3	10	843,898	*CNAG_04855*	hypothetical protein	A248S	G	T
TA8-4	03_11	308,737	*CNAG_02599*	predicted aldolase	N24N	A	G

Supplemental Figure 1

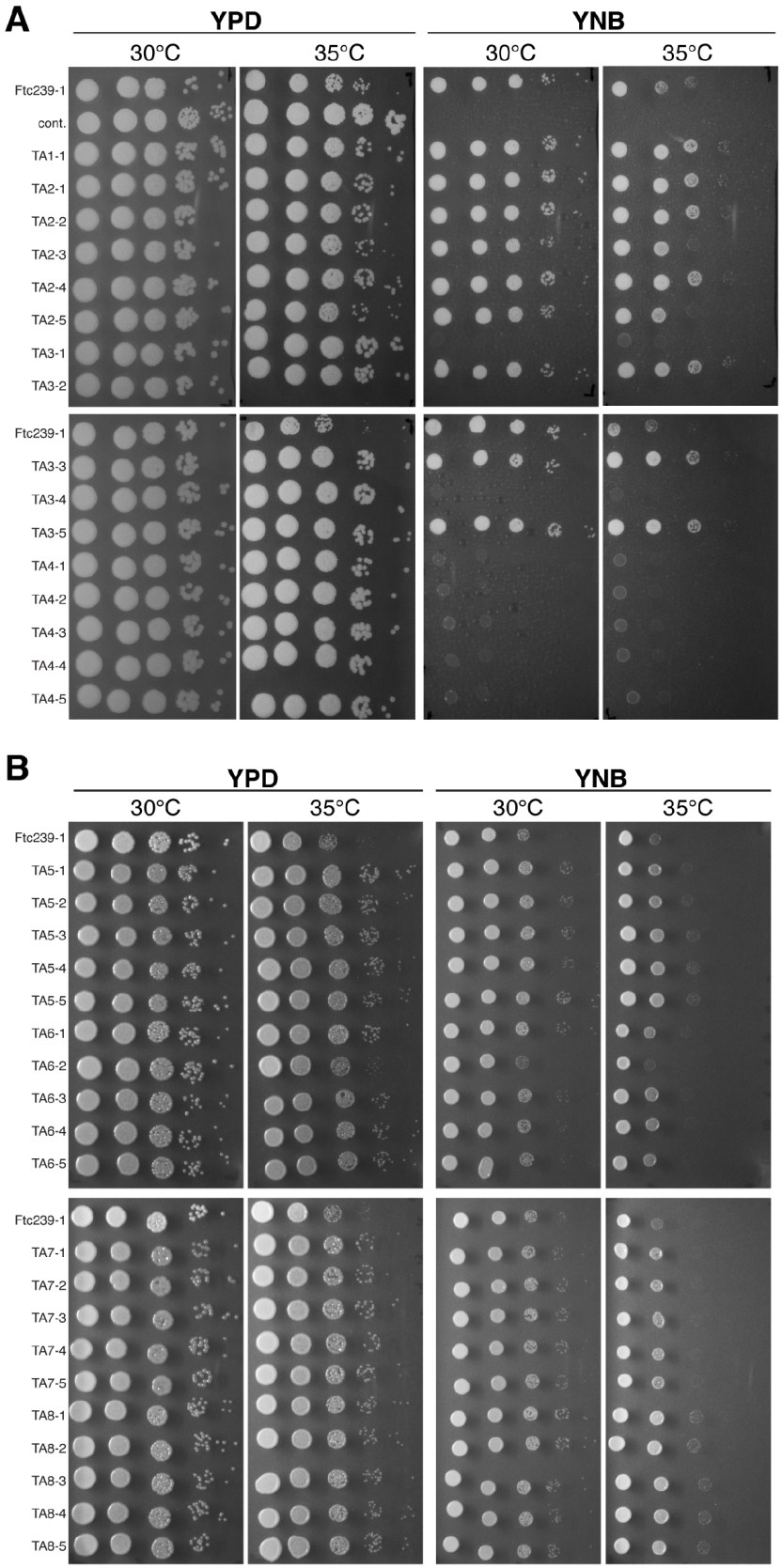

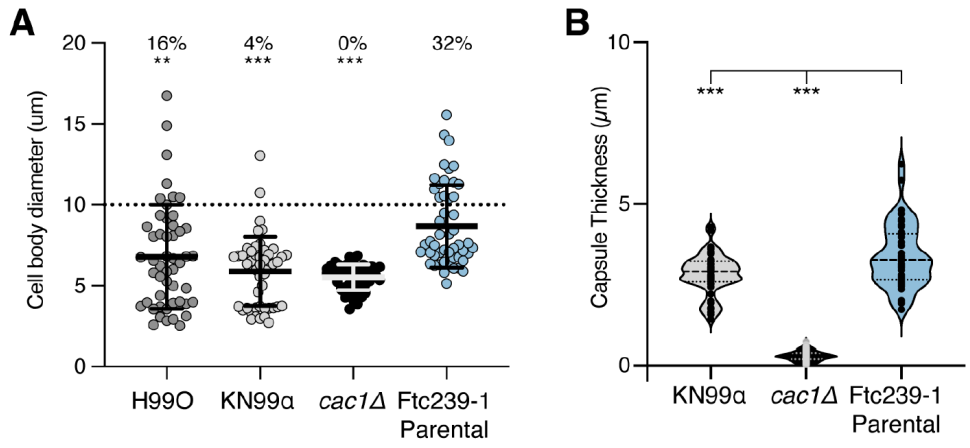
A
Cell body diameter (um)
20
15
10
5
0
16%
**
4%
***
0%
***
32%
H99O
KN99α
cac1Δ
Ftc239-1
Parental
B
Capsule Thickness (μm)
10
5
0
***
***
KN99α
cac1Δ
Ftc239-1
Parental

Supplemental Tables

Supplemental Table 1

Population	Colony #	Colony Appearance	Colony Size
Parental Ftc239-1		Smooth	Small
TA1	1	***Mucoid***	***Normal***
TA2	1	***Mucoid***	***Normal***
	2	***Mucoid***	***Normal***
	3	Smooth	***Normal***
	4	***Mucoid***	***Normal***
	5	Smooth	***Normal***
TA3	1	***Mucoid***	***Normal***
	2	***Mucoid***	***Normal***
	3	***Mucoid***	***Normal***
	4	***Mucoid***	***Normal***
	5	***Mucoid***	***Normal***
TA4	1	***Mucoid***	***Normal***
	2	***Mucoid***	***Normal***
	3	***Mucoid***	***Normal***
	4	***Mucoid***	***Normal***
	5	***Mucoid***	***Normal***

Supplemental Table 2

Population	Colony #	Colony Appearance	Colony Size
Parental Ftc239-1		Smooth	Small
TA5	1	Smooth	Small
	2	***Mucoid***	***Normal***
	3	***Mucoid***	Small
	4	***Mucoid***	Small
	5	Smooth	Small
TA6	1	Smooth	***Normal***
	2	Smooth	***Normal***
	3	Smooth	Small
	4	Smooth	***Normal***
	5	Smooth	Small
TA7	1	***Mucoid***	***Normal***
	2	***Mucoid***	***Normal***
	3	***Mucoid***	***Normal***
	4	***Mucoid***	***Normal***
	5	***Mucoid***	***Normal***
TA8	1	Smooth	***Normal***
	2	Smooth	***Normal***
	3	Smooth	Small
	4	Smooth	***Normal***
	5	Smooth	Small